Electronic Supplementary Information for

Piezochromic Luminescence of AIE-Active Molecular Co-crystals: Tunable Multiple Hydrogen Bonding and Molecular Packing

Bo Lu,[a] Yujian Zhang,*[b] Xiaogang Yang,[a] Kai Wang,[c] Bo Zou,*[c] and Dongpeng Yan*[a]

[a]Beijing Key Laboratory of Energy Conversion and Storage Materials, College of Chemistry, Beijing Normal University, Beijing 100875, People's Republic of China. *Email: yandongpeng001@163.com; yandp@bnu.edu.cn

[b]Department of Materials Chemistry, Huzhou University, East 2nd Ring Rd. No.759, Huzhou, 313000, People's Republic of China, Tel:+86-572-2322698. *Email: sciencezyj@foxmail.com

[c]State Key Laboratory of Superhard Materials, Jilin University, Qianjin Street 2699, Changchun, 130012, People's Republic of China. *Email: zoubo@jlu.edu.cn

Content:

Experimental section (preparation and characterization)

Materials. Tetrafluorohydroquinone (**B**), and 2,3,5,6-Tetrafluoro-4-hydroxy-benzoic acid (**C**) were purchased from J&K Scientific Co. Ltd. Chloroform ($CHCl_3$, analytical grade) and methanol (CH_3OH, analytical grade) were purchased from Beijing Chemical Co., China. All chemicals were of utilized without further purification. Moreover, **DCSB** was prepared according to the previous literature.[1,2]

Preparation of Co-crystals. The two new unreported co-crystals were prepared via a combined liquid-assisted grinding (**LAG**)[3] and solvent evaporation method. The ingredients of **DCSB** and co-former compounds were ground with different ratios (1:5 for **A-5B** and 1:2 for **A-2C**) in a Retsch MM200 mill for 15 minutes with several drops of $CHCl_3$. And the operating frequency of the ball mill machine was 20 Hz. Then the different kinds of ground powder were dissolved in the solvent of chloroform with adding methanol until the solution is clear and transparent. It is essential to control the evaporation rates of solutions carefully to ensure the quality and the size of the co-crystals. All the single crystals can be obtained in two or three weeks.

Instrumentation: Single crystal X-ray diffraction data for **A-5B** were collected by using an Eos, Gemini CCD diffractometer equipped with a graphite monochromator and an Oxford cryostream with MoKα radiation (λ = 0.71073 Å). The data for **A-5B** were obtained at 102.2 K by using the *ω*-scan method. The structure were solved by direct methods using the OLEX2 program[4] and refined by the full-matrix least-squares method on F^2. All non-hydrogen atoms were refined with anisotropic displacement parameters. The hydrogen atoms were located by the Fourier map method. Single crystal X-ray diffraction data for **A-2C** were collected using a Bruker SMART APEX CCD diffractometer equipped with graphite monochromatized Mo-Kα radiation (λ = 0.71073 Å) at room temperature using the *ω*-scan technique. Empirical absorption corrections were applied to the intensities using the SADABS program. The structures were solved using the SHELXS-2014 program[5] and refined by the full-matrix least-squares method on F^2 using the SHELXL-2014 program. All nonhydrogen atoms were refined anisotropically. The crystallographic data for **A-5B** and **A-2C** are listed in Table S1. Powder XRD patterns of all compounds were collected on a Shimadzu XRD-7000 automated diffraction system with Cu Kα radiation (λ = 1.5406 Å). Measurements were made in a 2θ range of 5-50° at room temperature with a step of 0.02° (2θ).The scan speed was 2 degree/min. The tube voltage and current were set to 40 kV and 30 mA, respectively. The fluorescence spectra for **A**, **A-5B** and **A-2C** were conducted using a Hitachi F-7000 (Hitachi High-Tech, Tokyo, Japan) fluorescence spectrometer under excitation of 368 nm with scan speed of 1200 nm/min. The PMT voltage was set as 600 V and the response time was set as auto mode. The PL quantum yield (PLQY) values were measured using a Teflon-lined integrating sphere (F-M101, Edinburgh, diameter: 150 mm and weight: 2 kg) in a FLS980 fluorescence spectrometer. The Time-resolved PL decay spectra of the samples were also performed on an Edinburgh FLS980 fluorescence spectrometer at room temperature. Photographs for single crystals were taken under an OLYMPUS IX71 fluorescence microscope. Solid UV-Vis absorption spectra were recorded on a Shimadzu UV-3600 spectrophotometer at room temperature.

High-pressure experiments. A piece of crystal was placed in the hole of a T301 steel gasket with a mixture of methanol and ethanol (V/V, 4/1) for pressure transmission medium (PTM) and ruby chip as pressure calibration. The *in-situ* PL spectra at high pressure were accomplished on an Ocean Optics QE65000 pectrometer in reflection mode. *In-situ* IR microspectroscopy of cocrystals powders at the high pressure was performed on a thermofisher IN10 FTIR with KBr as the PTM.

AIE experiments. Stock THF solution of **A-5B (or A-2C)** with a concentration of 2×10^{-4} M was prepared. Aliquots of the stock solution (400 μL for each one) were transferred to six 5 mL reagent bottles. For these six reagent bottles, different amounts of THF were added (3.6 mL, 3.2 mL, 2.4 mL, 1.6 mL, 0.8 mL and 0 mL). After appropriate amounts of THF were added, poor solvent water was added slowly under

vigorous shocking to furnish 2×10^{-5} M solutions with different water contents (0-90 vol %). The corresponding volumes of added water are 0 mL, 0.4 mL, 1.2 mL, 2.0 mL, 2.8 mL and 3.6 mL, respectively. The resulting solutions were placed for 24 hours. The fluorescence spectra for the resulting solutions were then recorded on an Edinburgh FLS980 fluorescence spectrometer under excitation of 368 nm with dwell time of 0.050 s. The excitation slit width was set as 4.00 and the emission slit width was set as 2.00. The UV-vis spectra for the resulting solutions were then performed on a Shimadzu UV-2450 spectrophotometer with medium-speed scan. The time-resolved PL decay spectra of the resulting solutions were also performed on an Edinburgh FLS980 fluorescence spectrometer at room temperature.

Fluorescent sensing experiments towards gas detection. The pH-responsive experiments were performed by alternate treatment of the powdered samples under the atmosphere conditions of ammonia solution (13 mol/L) and hydrochloric acid solution (12 mol/L), respectively. The variation in the fluorescence intensity with NH_3-HCl treatment vapor was recorded on Hitachi F-7000 fluorescence spectrometer under excitation of 368 nm with scan speed of 1200 nm/min. The PMT voltage was set as 600 V and the response time was set as auto mode.

Theoretical calculations on electrostatic potential distribution: The geometries of all molecules were fully optimized at the SCF level of theory using the Gaussian 09[6] suite of programs package. The ground state geometries have been optimized by using density functional theory (DFT) at B3LYP/6-31G* level.

Table S1. Crystal data and sturcture refinement for co-crystals **A-5B** and **A-2C**

Samples	**A-5B** (CCDC: 1842300)	**A-2C** (CCDC: 1842301)
Formula	$C_{54}H_{26}F_{20}N_2O_{10}$	$C_{38}H_{20}F_8N_2O_6$
Mr	1242.77	752.56
Temperature (K)	102.2	296(2)
Crystal system	triclinic	triclinic
Space group	$P\bar{1}$	$P\bar{1}$
Crystal size (mm)	0.12 × 0.09 × 0.03	0.25 × 0.25 × 0.20
a (Å)	6.0315(17)	9.3317(16)
b (Å)	7.416(2)	9.3436(16)
c (Å)	26.164(7)	10.5310(18)
α (°)	88.67(2)	63.940(3)
β (°)	88.29(2)	77.306(3)
γ (°)	85.06(2)	80.095(3)
V(Å^3)	1165.3(6)	801.7(2)
Z	1	1
D_{calc} (mg/m^3)	1.771	1.559
θ Range (°)	2.88-26.00	2.18-25.50
F (000)	624	382
Data/restraint/parameters	4578 / 0 / 393	2952 / 0 / 246
Reflections collected	8188	4307
Independent reflections	4578	2952
Goodness-of-fit on F^2	1.014	1.032
R_{int}	0.0457	0.0182
$R_1[I>2\sigma(I)]$	0.0544	0.0456
$wR_2[I>2\sigma(I)]$	0.0882	0.1137
R_1(all data)	0.0983	0.0770
wR_2(all data)	0.1127	0.1379
Residuals(e Å^{-3})	0.308, -0.318	0.197, -0.207

$R_1 = \Sigma||F_o| - |F_c||/\Sigma|F_o|$, $wR_2 = [\Sigma w(F_o^2 - F_c^2)^2/\Sigma w(F_o^2)^2]^{1/2}$

Table S2. Photophysical properties of **A**, **A-5B** and **A-2C**

Samples	PL(nm)	Φ_F(%)	<τ> (ns)	$k_r/10^8$ s^{-1}	$k_{nr}/10^8$ s^{-1}
A	442	79.2	1.973	4.0	1.1
A-2C	458	60.5	2.065	2.9	1.9
A-5B	498	51.2	7.954	0.64	0.61

$<\tau> = \sum A_j\tau_j^2 / \sum A_j\tau_j$, j=1,2,3..., $\Phi_F = <\tau> \times k_r$, where <τ> is the fluorescence lifetime, Φ_F is the quantum yield, and k_r is the radiative deactivation rate. k_r and k_{nr} were obtained by $k_r = \Phi_F/<\tau>$; $k_{nr} = 1-\Phi_F/<\tau>$.

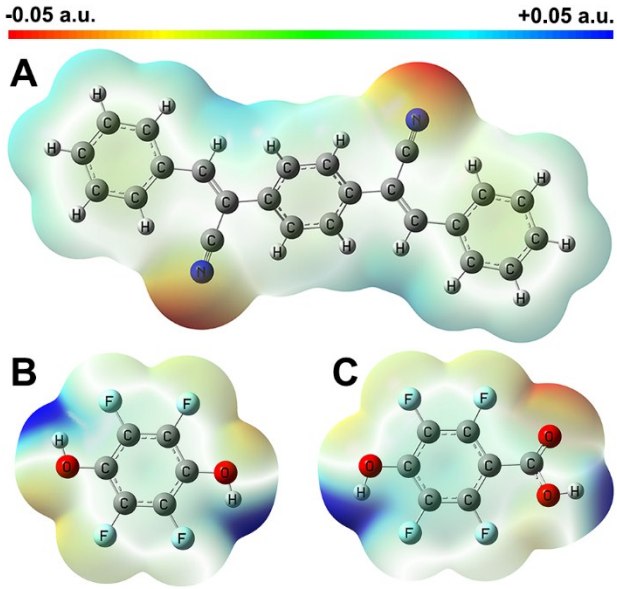

Figure S1. The calculated electrostatic potential distribution maps: 4-bis(1-cyano-2-phenylethenyl)benzene (**DCSB**, **A**) ; Tetrafluorohydroquinone (**B**) and 2,3,5,6-Tetrafluoro-4-hydroxy-benzoic (**C**). Blue: electropositive; red: electronegative; green: electroneutral.

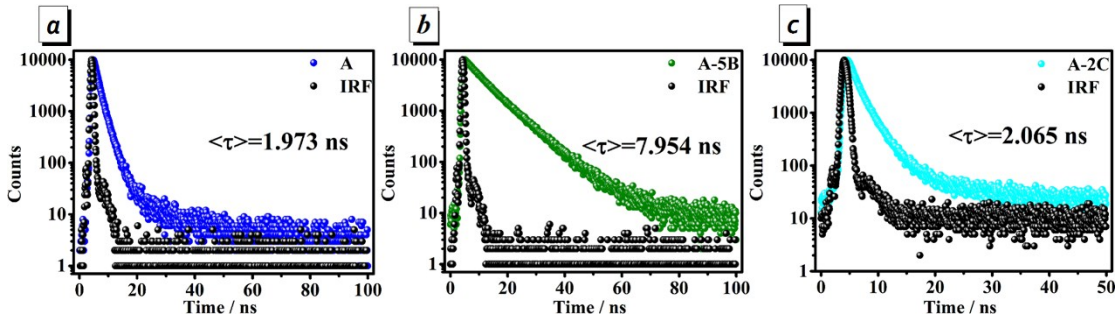

Figure S2. Time-resolved fluorescence decay curves of the **A**, **A-5B** and **A-2C**.

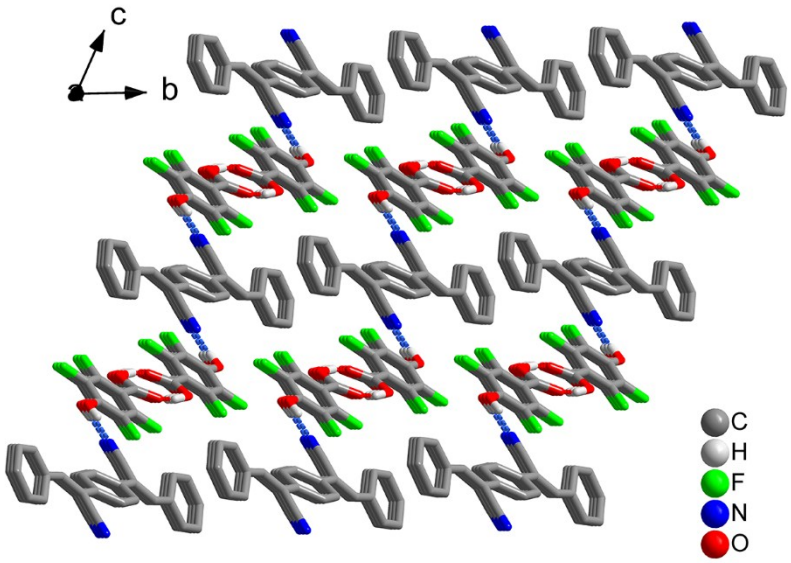

Figure S3. In **A-2C**, the **DCSB** molecules were assembled with a pair of **C** molecules alternately through O-H•••N hydrogen bonds (blue dash, 2.012 Å) to form 1D chain structures. (red dash, O-H•••O hydrogen bonds)

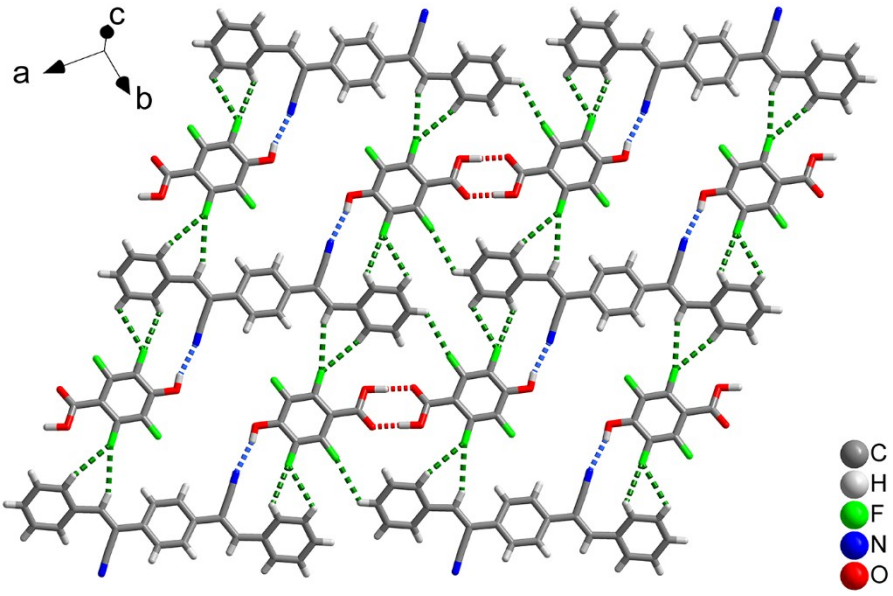

Figure S4. In **A-2C**, the adjacent 1D chains became interconnected by C-F•••H hydrogen bonds to form 2D 'molecular sheets' structures. (blue dash, O-H•••N hydrogen bonds; red dash, O-H•••O hydrogen bonds; green dash, C-H•••F hydrogen bonds).

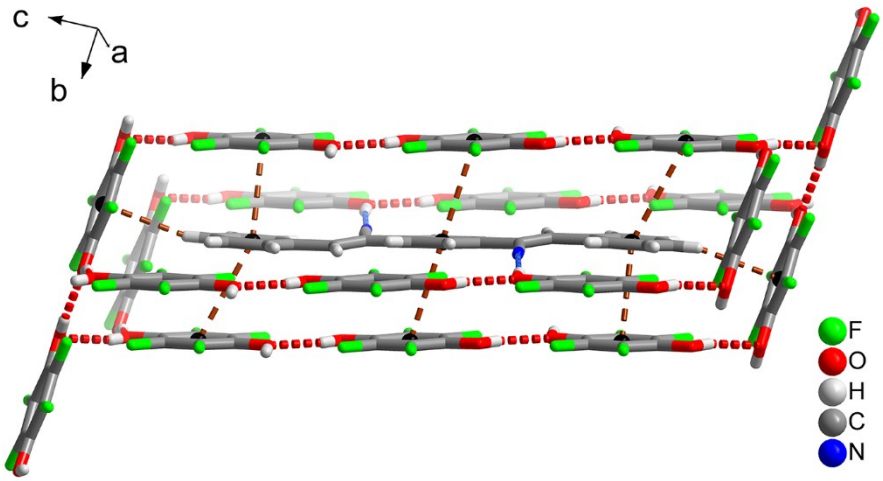

Figure S5. In **A-5B**, one **DCSB** molecule was closely encircled by two crosswise annular architectures.

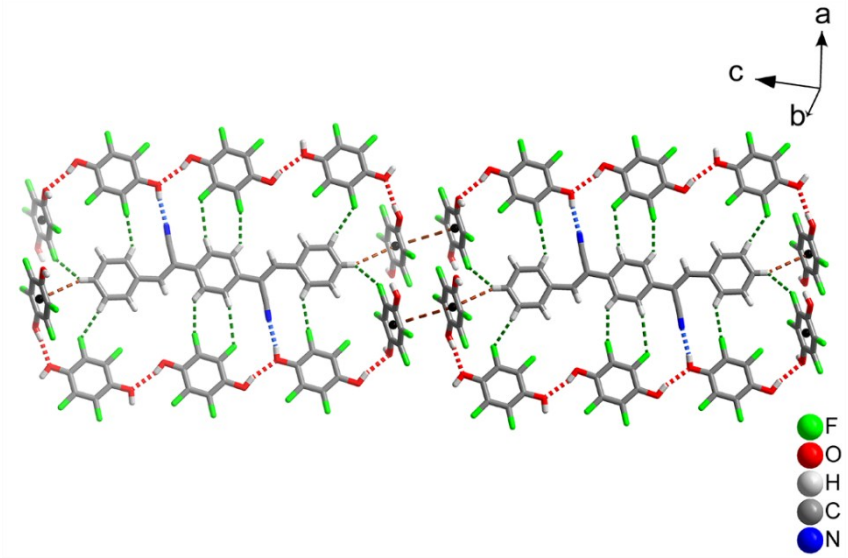

Figure S6. In **A-5B**, two neighboring transverse molecular rings were connected with each other by the face-to-face interactions (3.14 Å) between adjacent **B** molecules.

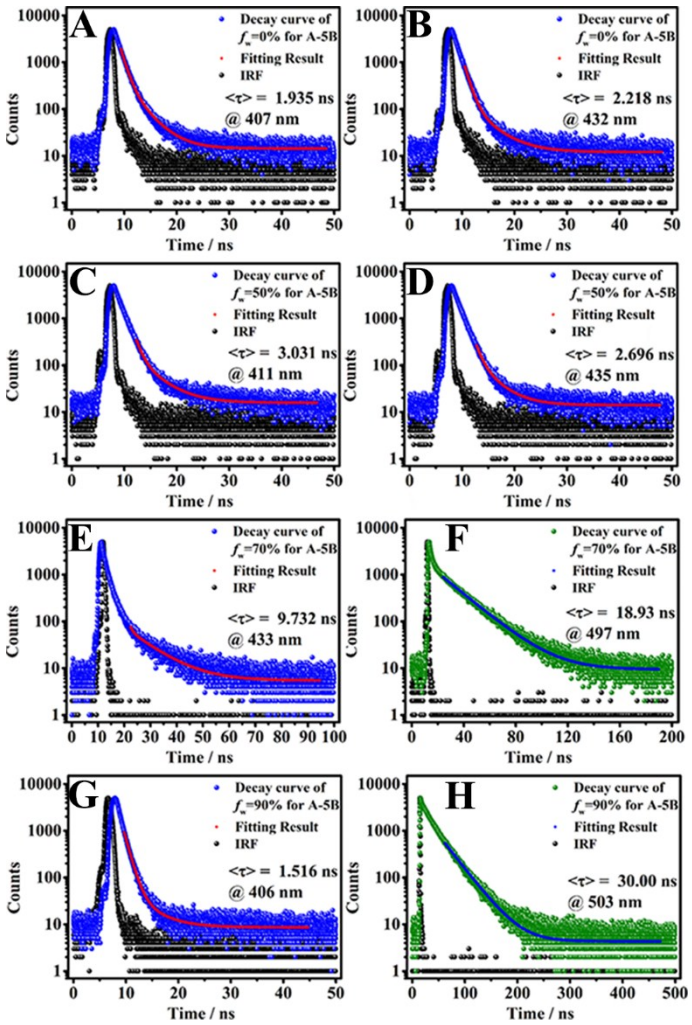

Figure S7. Time-resolved fluorescence decay curves of the **A-5B** in THF-H_2O mixture solutions with different water fractions (f_w = 0%, 50%, 70% and 90%).

Table S3. Fluorescence lifetimes (τ) of **A-5B** in THF-H_2O mixture solutions with different water fractions (f_w = 0-90%)

Samples	Wavelength (nm)	τ_1 (ns)	A_1 (%)	τ_2 (ns)	A_2 (%)	<τ> (ns)	χ^2
f_w=0%	407	1.000	57.51	3.200	42.49	1.935	1.293
	432	1.000	59.41	4.000	40.59	2.218	1.288
f_w=50%	411	1.000	32.30	4.000	67.70	3.031	1.211
	435	1.000	32.17	3.500	67.83	2.696	1.276
f_w=70%	433	1.000	2.98	10.00	97.02	9.732	1.251
	497	18.93	100	-	-	18.93	1.140
f_w=90%	406	1.000	82.80	4.000	17.20	1.516	1.149
	503	30.00	100	-	-	30.00	1.274

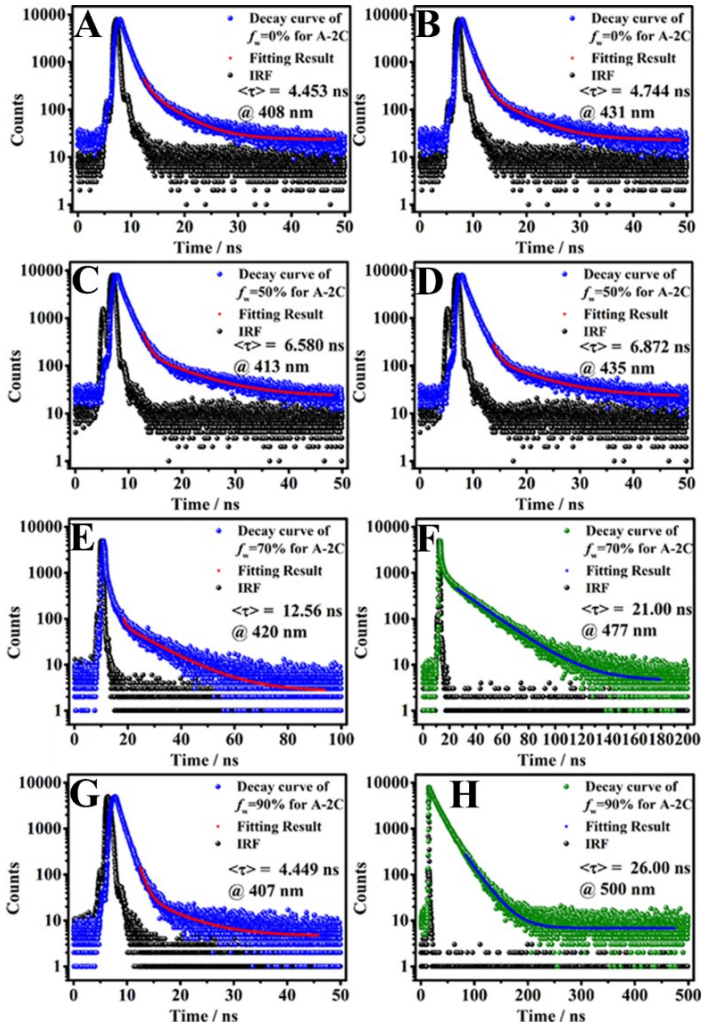

Figure S8. Time-resolved fluorescence decay curves of the **A-2C** in THF-H_2O mixture solutions with different water fractions (f_w = 0%, 50%, 70% and 90%).

Table S4. Fluorescence lifetimes (τ) of **A-2C** in THF-H_2O mixture solutions with different water fractions (f_w = 0%, 50%, 70% and 90%)

Samples	Wavelength (nm)	τ_1 (ns)	A_1 (%)	τ_2 (ns)	A_2 (%)	<τ> (ns)	χ^2
f_w=0%	408	1.000	13.68	5.000	86.32	4.453	1.199
	431	1.000	25.11	6.000	74.89	4.744	1.273
f_w=50%	413	1.000	20.28	8.000	79.72	6.580	1.233
	435	1.000	16.12	8.000	83.88	6.872	1.111
f_w=70%	420	1.000	3.70	13.00	96.30	12.56	1.179
	477	21.00	100	-	-	21.00	1.220
f_w=90%	407	1.000	37.29	6.500	62.71	4.449	1.277
	500	26.00	100	-	-	26.00	1.269

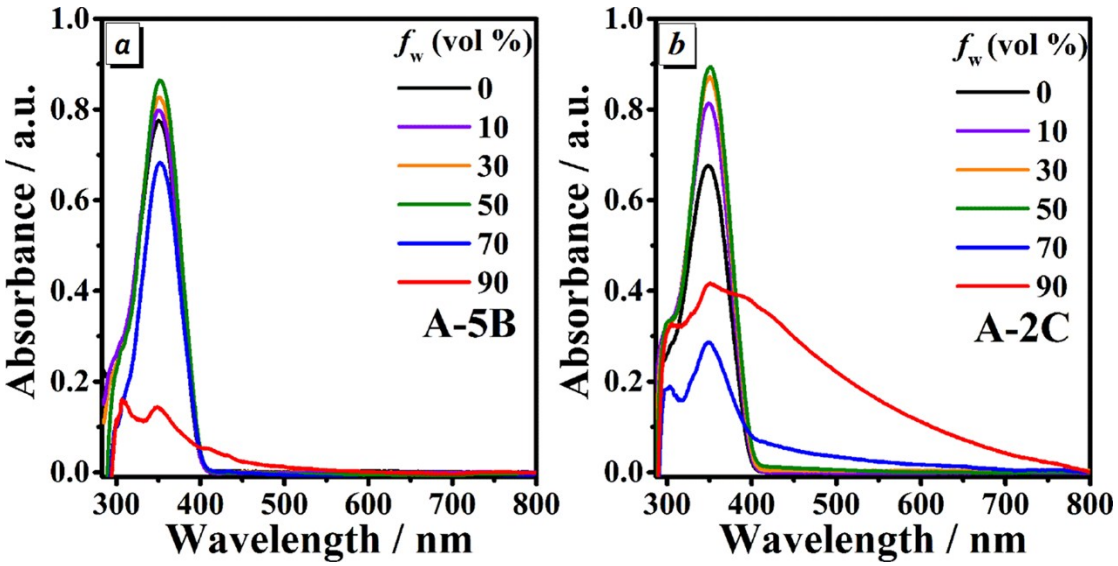

Figure S9. UV-Vis spectra of **A-5B** (a) and **A-2C** (b) in THF-H_2O mixtures with different water fractions (f_w = 0-90%). Solution concentration: 0.02 mM.

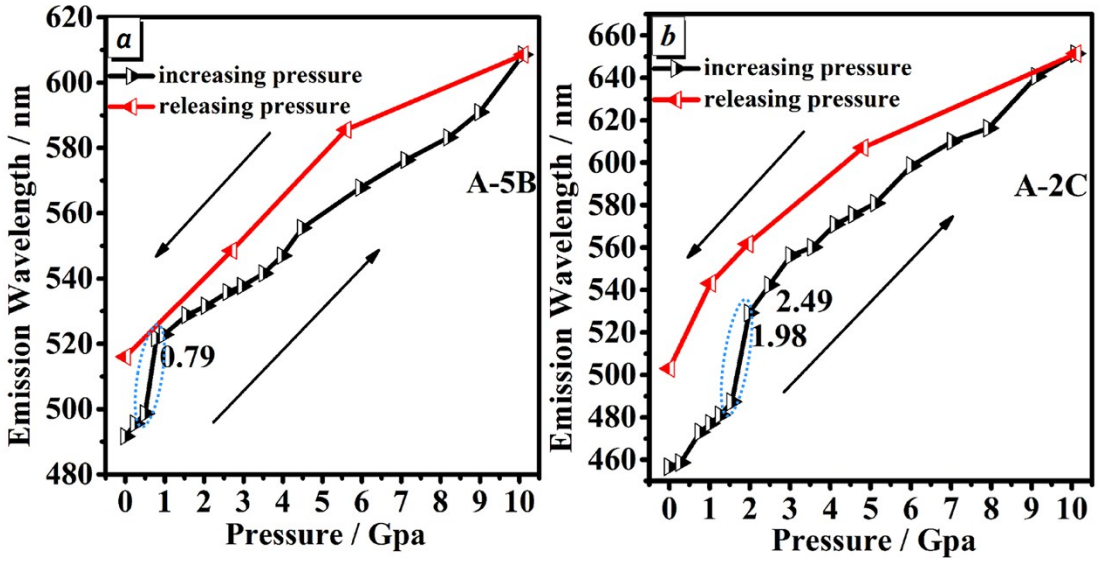

Figure S10. Plot showed the corresponding relationship between the wavelength shift of emission dominant peak values and the pressure values during the process of applying pressure (black lines) and releasing pressure (red lines) for **A-5B** (a) and **A-2C** (b) samples.(The blue dotted areas represent the process of drastic change for emission peak wavelength)

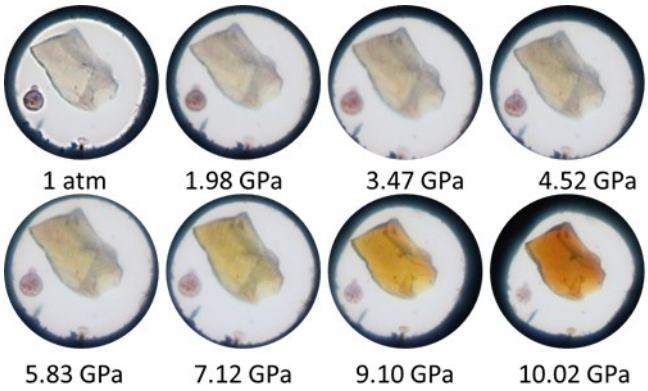

Figure S11. Photographs of the **A-2C** cocrystal as gradually increasing hydrostatic pressures (from atmospheric pressure to 10.02 Gpa), taken under day light.

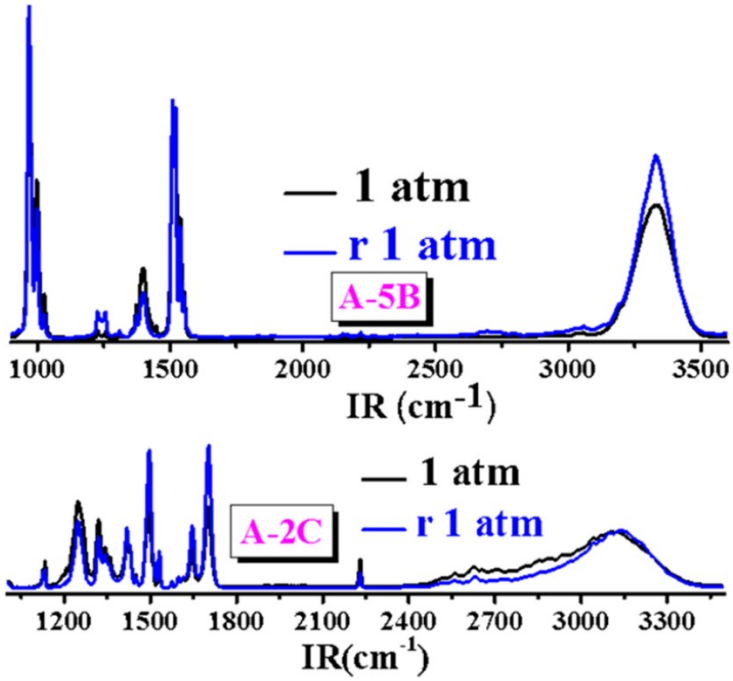

Figure S12. Before applying pressure (black lines) and after releasing the applied pressure (blue lines) under normal pressure (1 atm), the *in-situ* IR spectroscopy for **A-5B** and **A-2C** samples.

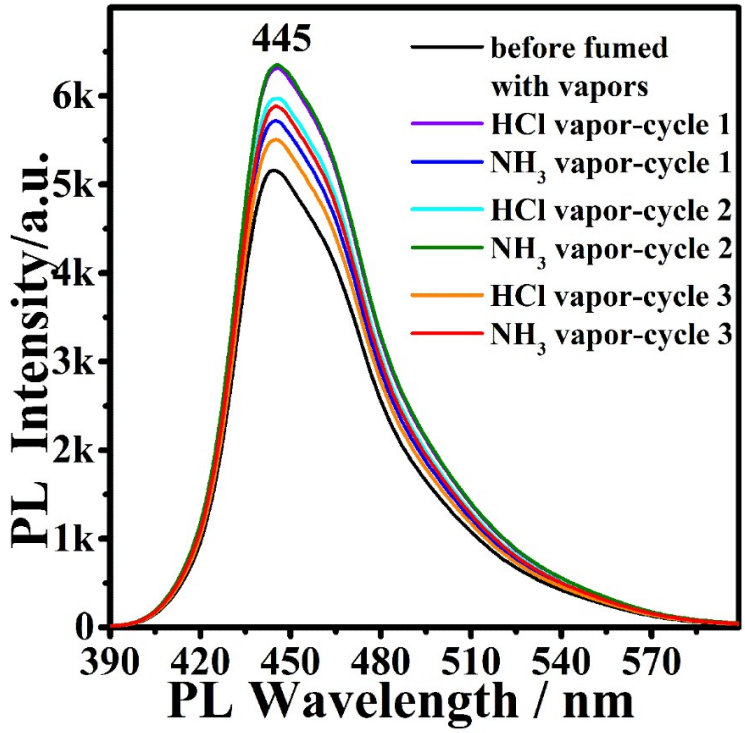

Figure S13. Fluorescence spectra for pristine **DCSB** sample before and after fuming with HCl vapor or NH_3 vapor, alternately.

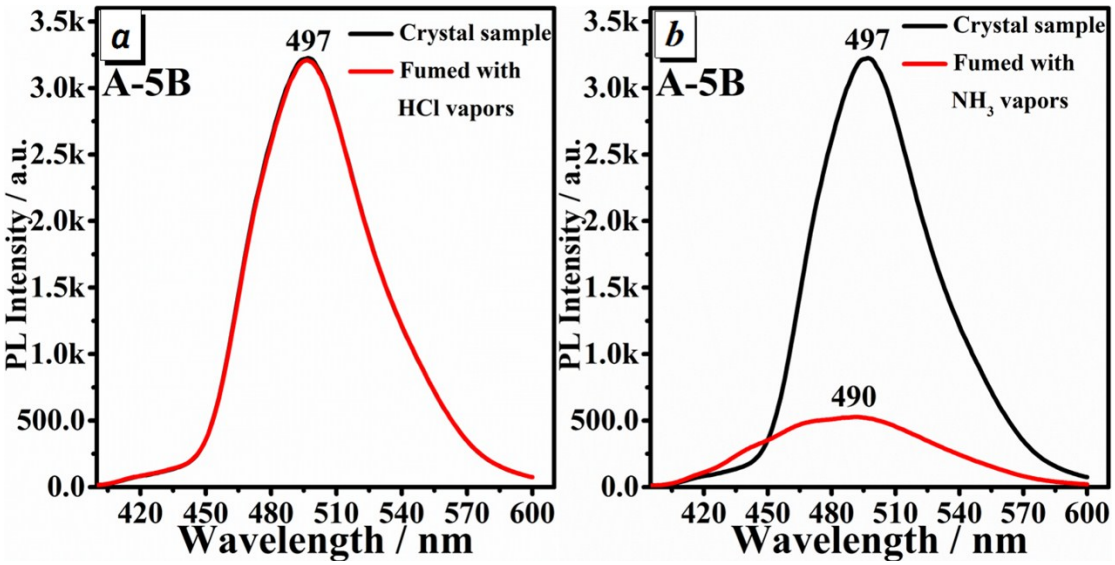

Figure S14. Fluorescence spectra for **A-5B** sample before (black lines) and after (red lines) fuming with HCl vapor (a) and NH_3 vapor (b), respectively.

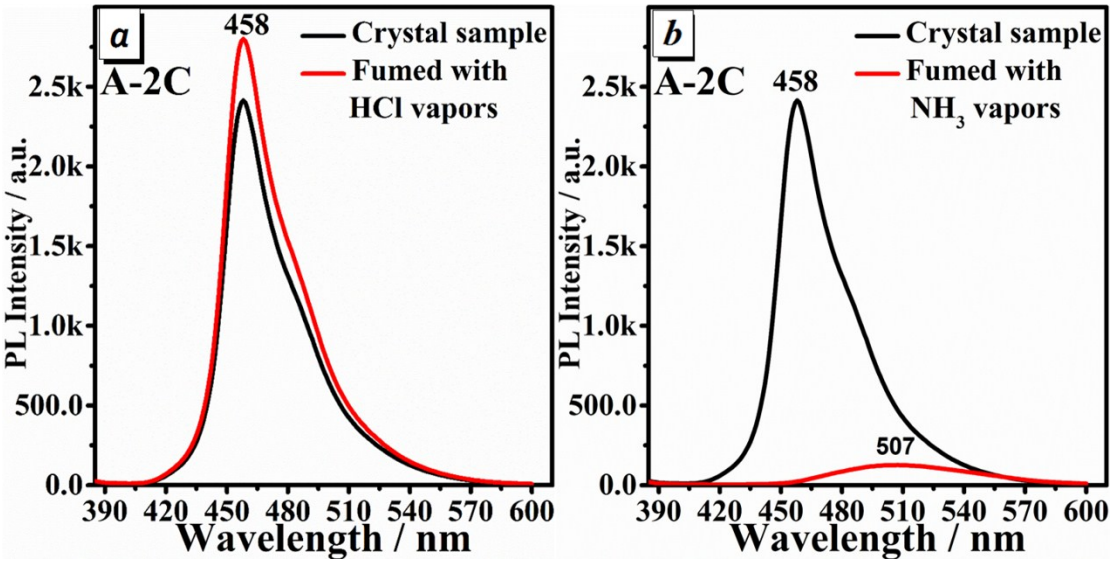

Figure S15. Fluorescence spectra for **A-2C** sample before (black lines) and after (red lines) fuming with HCl vapor (a) and NH_3 vapor (b), respectively.

References

1 S. -J Yoon and S. Y. Park, *J. Mater. Chem*., 2011, **21**, 8338-8346.

2 Y. Zhang, S. Li, G. Pan, H. Yang, M. Qile, J. Chen, Q. Song and D. Yan, *Sens. Actuators, B*, 2018, **254**, 785-794.

3 T. Friščić, A. V. Trask, W. Jones and W. D. S. Motherwell, *Angew. Chem. Int. Ed.*, 2006, **118**, 7708-7712.

4 O. V. Dolomanov, L. J. Bourhis, R. J. Gildea, J. A. K. Howard and H. Puschmann, *J. Appl. Crystallogr.*, 2009, **42**, 339-341.

5 G. M. Sheldrick, Program for the crystal structure solution; University of Göttingen: Göttingen, Germany, 2014.

6 M. J. Frisch, G. W. Trucks, H. B. Schlegel, G. E. Scuseria, M. A. Robb, J. R. Cheeseman, G. Scalmani, V. Barone, B. Mennucci, G. A. Petersson, et al. Gaussian 09, revision A.1; Gaussian, Inc.: Wallingford, CT, 2009.